Hindawi Publishing Corporation
International Journal of Photoenergy
Volume 2013, Article ID 570587, 9 pages
http://dx.doi.org/10.1155/2013/570587

Research Article

Solar Photocatalytic Degradation of Bisphenol A on Immobilized ZnO or TiO_2

Andreas Zacharakis,[1] Efthalia Chatzisymeon,[1] Vassilios Binas,[2] Zacharias Frontistis,[1] Danae Venieri,[1] and Dionissios Mantzavinos[1,3]

[1] *Department of Environmental Engineering, Technical University of Crete, Polytechneioupolis, 73100 Chania, Greece*
[2] *Institute of Electronic Structure and Laser (IESL), FORTH, P.O. Box 1527, Vassilika Vouton, 71110 Heraklion, Greece*
[3] *Department of Chemical Engineering, University of Patras, Caratheodory 1, University Campus, 26504 Patras, Greece*

Correspondence should be addressed to Dionissios Mantzavinos; mantzavinos@chemeng.upatras.gr

Received 30 May 2013; Accepted 14 July 2013

Academic Editor: Christos Trapalis

The removal of bisphenol A (BPA) under simulated solar irradiation and in the presence of either TiO_2 or ZnO catalysts immobilized onto glass plates was investigated. The effect of various operating conditions on degradation was assessed including the amount of the immobilized catalyst (36.1–150.7 mg/cm^2 for TiO_2 and 0.5–6.8 mg/cm^2 for ZnO), initial BPA concentration (50–200 μg/L), treatment time (up to 90 min), water matrix (wastewater, drinking water, and pure water), the addition of H_2O_2 (25–100 mg/L), and the presence of other endocrine disruptors in the reaction mixture. Specifically, it was observed that increasing the amount of immobilized catalyst increases BPA conversion and so does the addition of H_2O_2 up to 100 mg/L. Moreover, BPA degradation follows first-order reaction kinetics indicating that the final removal is not practically affected by the initial BPA concentration. Degradation in wastewater is slower than that in pure water up to five times, implying the scavenging behavior of effluent's constituents against hydroxyl radicals. Finally, the presence of other endocrine disruptors, such as 17α-ethynylestradiol, spiked in the reaction mixture at low concentrations usually found in environmental samples (i.e., 100 μg/L), neither affects BPA degradation nor alters its kinetics to a considerable extent.

1. Introduction

Endocrine disrupting compounds (EDCs) constitute an important class of emerging environmental contaminants, which pose an increasing threat to aquatic organisms, as well as to human health [1]. In particular, the exposure to EDCs has been linked with altering functions of the endocrine system in male fish such as vitellogenin induction and feminized reproductive organs [2]. Moreover, the increasing incidence of cancer and the hypothesis of a decreasing reproductive fitness of men are thought to be attributed to endocrine disruptors. Among various EDCs, bisphenol A (BPA) is well-known for its interference with the endocrine system of living beings [3, 4]. BPA is widely used in the manufacturing of numerous chemical products, such as CDs, DVDs, drink containers, electrical and electronic equipment, and protective coatings [1, 5]. These substances enter municipal wastewater treatment plants (WWTPs) through either human excretion or their direct disposal in the sewage system. Currently, when EDCs enter conventional biological WWTP, only a small amount of these chemicals are removed via biodegradation processes because most of them are xenobiotics and thus non-biodegradable [6]. Therefore, the majority of EDCs remain soluble in the effluent, and they are discharged to aquatic bodies. In the last decade, several studies have confirmed the occurrence of EDCs at the level of ng/L–μg/L in inland waters (rivers and streams) and wastewaters (outlets of municipal and industrial WWTPs) worldwide [7–11]. Not only this, but it has been found that these compounds can pose a potential danger to fish and other aquatic organisms, even at low concentrations of 0.1–10 ng/L [12]. Thus, it is necessary to look further on the removal mechanisms, in order to improve

the efficiency of the existing treatment systems and to develop new and reliable treatment strategies to remove EDCs from wastewaters.

Semiconductor photocatalysis using solar radiation as the source of photons for the activation of the catalyst has received considerable attention over the past several years. Several heterogeneous photocatalysts have been investigated, and, amongst them, the use of TiO_2 under ultraviolet and/or visible light has extensively been researched. Another photocatalyst that absorbs over a large fraction of the solar spectrum is ZnO with a gap energy of 3.2 eV. The photocatalytic mechanism of ZnO is similar to that of TiO_2 [13]. Moreover, solar photocatalysis is considered as a cost-effective and sustainable treatment technique due to the utilization of solar energy (an abundant source of energy). However, the biggest problem with slurry photocatalysis has been recognized to be the need for a posttreatment recovery step [14, 15]. Therefore, research has been conducted to produce catalysts on supports that would keep the catalyst powder out of the treated water and sufficiently reduce even more the cost of the photocatalytic process, since there will be no need for catalyst aftertreatment. So far, few studies have dealt with the treatment of EDCs by means of TiO_2 or ZnO catalysts immobilized onto supports, such as glass [4, 16], PTFE mesh sheets [17], titanium substrates [18, 19], and polyurethane foam cubes [20].

Hence, in this work, the efficacy of solar photocatalytic process to remove BPA from aqueous environmental samples was investigated. For this purpose, two different photocatalytic materials, namely, ZnO and TiO_2, were immobilized onto appropriate glass substrate by means of a heat attachment technique. The effect of various operating parameters, such as the immobilized catalyst amount, the initial BPA concentration, the treatment time, the water matrix, the addition of H_2O_2, and the presence of other organic substances, on process efficiency, was investigated.

2. Materials and Methods

2.1. Materials. BPA and 17α-ethynylestradiol (EE2) were purchased from Sigma-Aldrich, while ZnO (≥99%, particle size < 100 nm, 15–25 m^2/g BET surface area) and TiO_2-P25 (anatase : rutile 75 : 25, 21 nm primary crystallite particle size, 50 m^2/g BET surface area) were purchased from Fluka and Degussa-Evonik Corp., respectively. The water matrix was either of the following three: (i) wastewater (WW) collected from the outlet of the secondary treatment of the municipal WWTP of Chania, W. Crete, Greece; (ii) commercially available bottled water, which will be referred to in the text as drinking water (DW); and (iii) ultrapure water (UPW) at pH = 6.1 taken from a water purification system (EASYpureRF-Barnstead/Thermolyne, USA). The main properties of WW and DW are given in Table 1.

2.2. Catalyst Preparation. The ZnO or TiO_2 catalyst powders were immobilized on glass plates (1.5 cm × 1.5 cm) by a heat attachment method. Analytically, the glass plates were first treated with a 38% HF solution and then washed with 0.01 M NaOH in order to increase the number of OH groups and achieve better contact of the catalyst on glass plates [14]. Moreover, a suspension of 8 g/L catalyst in distilled water was prepared. This suspension was sonicated at 80 kHz for 120 min in order to improve the dispersion of the solid catalyst in water. Afterwards, the sonicated catalyst solution was poured on the glass plates at various volumes, ranging from some μL to about 10 mL and then placed in an oven at 120°C for 60 min. After drying, the glass plates were calcined at 500°C for 180 min. Finally, the glass plates were washed with distilled water to remove the loosely attached catalytic particles.

Table 1: Properties of wastewater and drinking water matrices used in this study.

Parameter	Wastewater	Drinking water
pH	8	7.7
TOC (mg/L)	7.8	0.3
COD (mg/L)	24	ND
Conductivity (μs/cm)	820	329
HCO_3^- (mg/L)	190	188
Cl^- (mg/L)	220	<5
NO_2^- (mg/L)	57	<0.09
NO_3^- (mg/L)	26	<5

ND: not determined.

2.3. Catalyst Characterization Techniques. The crystal structure, particle size, and morphology were examined with a powder X-ray diffraction (XRD) system and scanning electron microscopy (SEM), respectively. XRD patterns were collected on a Rigaku D/MAX-2000H rotating anode diffractometer (Cukα radiation) equipped with a secondary pyrolytic graphite monochromator operating at 40 kV and 80 mA over the 2θ collection range of 10–80°. The scan rate was 0.05/min with a step size of 0.01. Surface morphology of the catalytic plates was carried out on a JEOL JSM-6400V SEM instrument.

2.4. Photocatalytic Experiments. Photocatalytic experiments were performed using a solar simulator (Newport, model 96000) equipped with a 150 W xenon ozone-free lamp and an Air Mass 1.5 Global Filter (Newport, model 81094), simulating solar radiation reaching the surface of the earth at a zenith angle of 48.2°.

The incident radiation intensity on the photochemical reactor in the UV region of the electromagnetic spectrum was measured actinometrically using 2-nitrobenzaldehyde (purchased from Sigma-Aldrich) as the chemical actinometer [21], and it was found to be 16.5 10^{-5} einstein/m^2. In a typical photocatalytic run, 64 mL of the water matrix spiked with the appropriate amount of the organic substance was fed in a cylindrical pyrex cell and the ZnO or TiO_2 catalytic plate was added, while the cell was open to the atmosphere. The solar simulator was placed on top of the liquid surface, while the catalytic glass plate was held by a Ti support dipped into

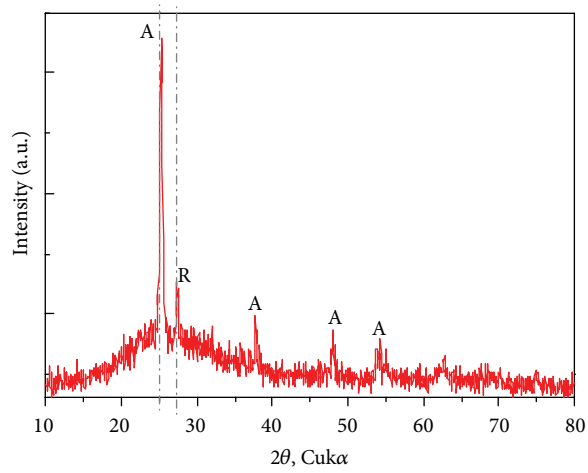

FIGURE 1: XRD pattern of the TiO_2 immobilized particles on glass plate (A: anatase; R: rutile).

the reaction mixture. Samples of about 1 mL were periodically taken from the cell and analyzed as follows.

2.5. Analytical Techniques. High-performance liquid chromatography (Alliance 2690, Waters) was employed to monitor the concentrations of BPA and EE2. Separation was achieved on a Luna C-18(2) column (5 μm, 250 mm × 4.6 mm) and a security guard column (4 mm × 3 mm), both purchased from Phenomenex. The mobile phase consists of 35 : 65 UPW : acetonitrile eluted isocratically at 1 mL/min and 30°C, while the injection volume was 100 μL. Detection was achieved through a fluorescence detector (Waters 474), in which the excitation wavelength was 280 nm and the emission wavelength was 305 nm. Under these conditions, the retention time for BPA was 4.3 min, the limit of detection was 0.68 μg/L, and the limit of quantitation was 2.32 μg/L; the respective values for EE2 were 5.1 min, 0.63 μg/L, and 2.11 μg/L. Residual H_2O_2 concentration was monitored using Merck peroxide test strips in the range 0–100 mg/L. Changes in effluent pH during photocatalytic treatment were checked using a Toledo 225 pH meter.

3. Results and Discussion

3.1. TiO_2 Catalyst Plates. Figure 1 shows XRD pattern of the TiO_2 immobilized particles on glass plate subjected to heat treatment at 500°C for 3 h. Peaks at 2θ values of 25° and 27° correspond to the anatase (101) and rutile (110) planes, respectively. The crystalline size (D) was calculated at 17 nm using the Scherrer equation:

$$D = \frac{k\lambda}{\beta \cos\theta}, \quad (1)$$

where k is a constant equal to 0.9, λ is the wavelength of characteristics X-ray applied (0.15418 nm), β is the full width at half maximum of the anatase (101) peak obtained by XRD, and θ is the Bragg angle.

The phase content of TiO_2 particles can be calculated as follows:

$$f_A = \frac{1}{1 + I_R/0.79I_A}, \quad (2)$$

where f_A is the content of anatase, and I_A and I_R are the integrated intensities of the anatase (101) and rutile (110) peaks, respectively. The TiO_2 catalytic plate mainly consists of the anatase phase with mirror rutile phase (70 : 30).

Figure 2 shows SEM images of the immobilized catalytic particles on glass plates with different amounts of TiO_2 in the range 81.3–339.2 mg (36.1–150.7 mg/cm^2). The TiO_2 layer is homogeneous with a porous surface, while the morphology of TiO_2 particles is amorphous. As the amount of TiO_2 increases the homogeneity increases and so does the film thickness in the range 2–6 μm.

The effect of increasing the amount of immobilized TiO_2 on BPA removal is shown in Figure 3; the 90 min conversion increases from 60% to 80% as TiO_2 increases from 36.1 to 150.7 mg/cm^2, and this is expected since more catalyst surface sites are available for reaction at higher catalyst loadings. An additional run was performed in the absence of catalyst yielding only 15% photolytic removal after 90 min. Since TiO_2 in slurry has extensively been used for photocatalytic purposes, an extra run was carried out to compare the efficiencies of slurry and immobilized catalysts. Hence, 0.65 mg TiO_2 powder was added to the reaction mixture, and complete removal of 100 μg/L BPA could be achieved after 35 min of reaction (data not shown). This shows that slurry catalysts, even at extremely low concentrations, yield higher reaction rates than the immobilized systems, presumably due to lower mass transfer limitations.

3.2. ZnO Catalyst Plates. Figure 4 shows XRD pattern of the ZnO immobilized particles on glass plate subjected to heat treatment at 500°C for 3 h. The sharp intense peaks of ZnO confirm the good crystalline nature of ZnO and form (100), (002), (101), (102), (110), (103), (200), and (112) reflections of hexagonal ZnO. The size of the particles was calculated at 47 nm using (1).

Figure 5 shows SEM images of the immobilized catalytic particles for the fresh and used ZnO. Moreover, the initial glass plate, as well as the HF-treated surface, is shown. It is evident that the glass surface becomes rough after acid treatment (Figure 5(b)), thus facilitating catalyst attachment. Figure 5(c) shows the dispersion of fresh ZnO onto the glass surface, where agglomeration of the particles takes place to some extent. Conversely, Figure 5(d) shows the SEM image of a plate that has been employed for more than 30 h of photocatalytic experiments under various conditions (including runs with wastewater). It is observed that particles dispersion is more homogeneous than that of the fresh plate and this is probably due to the presence of several organic and/or inorganic impurities accumulated onto the surface during its photocatalytic use. The film thickness is in the range 2–4 μm.

The effect of increasing ZnO loading in the range 1.2–15.3 mg (0.5–6.8 mg/cm^2) on BPA removal is shown in

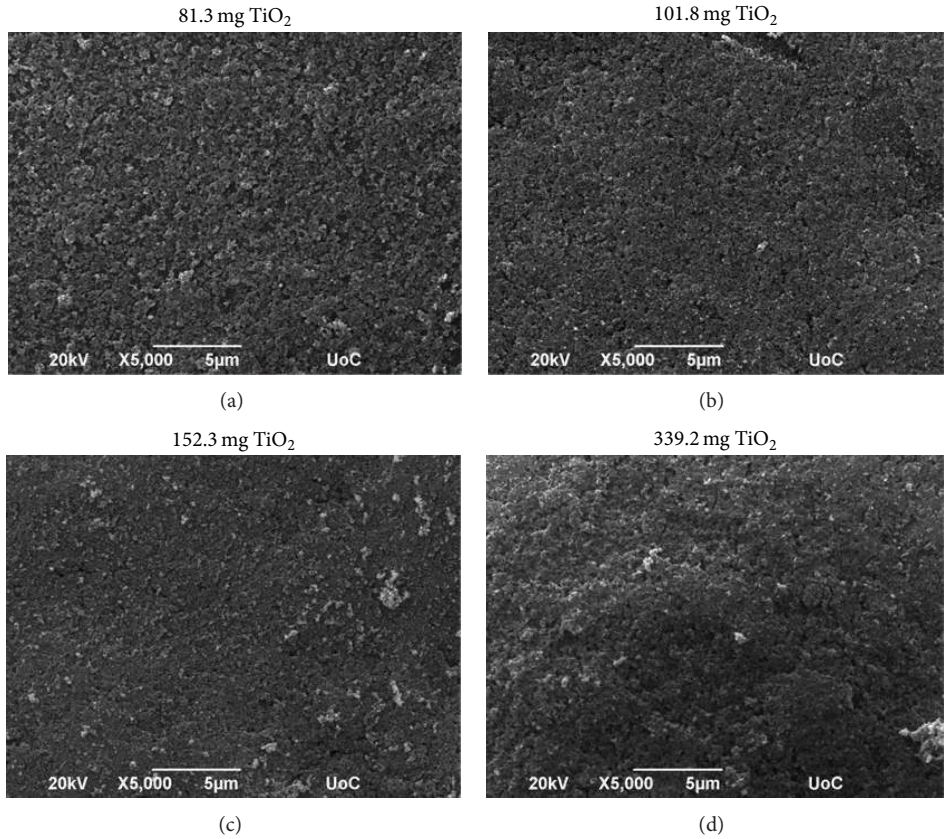

Figure 2: SEM images of TiO_2 immobilized particles on glass plate with increasing amount of catalyst from 81.3 to 339.2 mg (36.1 to 150.7 mg/cm^2).

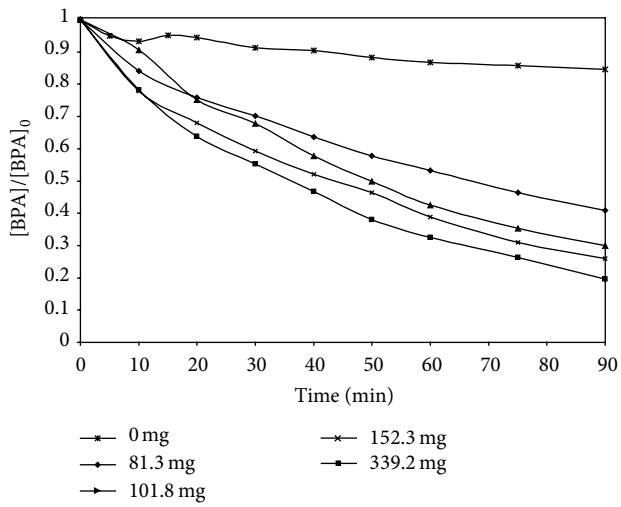

Figure 3: Effect of TiO_2 loading on the conversion of 100 μg/L BPA in UPW.

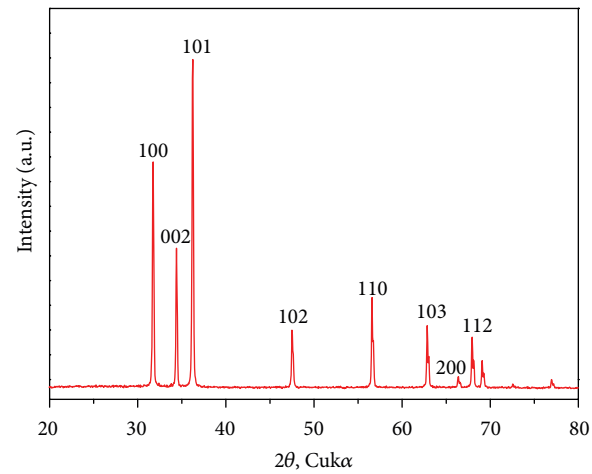

Figure 4: XRD pattern of the ZnO immobilized particles on glass plate.

Figure 6, where the 90 min conversion is enhanced from 52% to 90%. Notably, for ZnO loadings between 1.6 and 2.5 mg/cm^2, BPA degradation remains practically unchanged at about 65%.

Another interesting finding is that for the same volume of the catalyst aqueous suspension (i.e., from 200 μL to 10 mL), the quantity of ZnO attached onto the glass support is 1-2 orders of magnitude lower than that of TiO_2. This is due to the fact that TiO_2 is known to have more hydroxyl anions on its surface than ZnO, thus enhancing the adhesion of

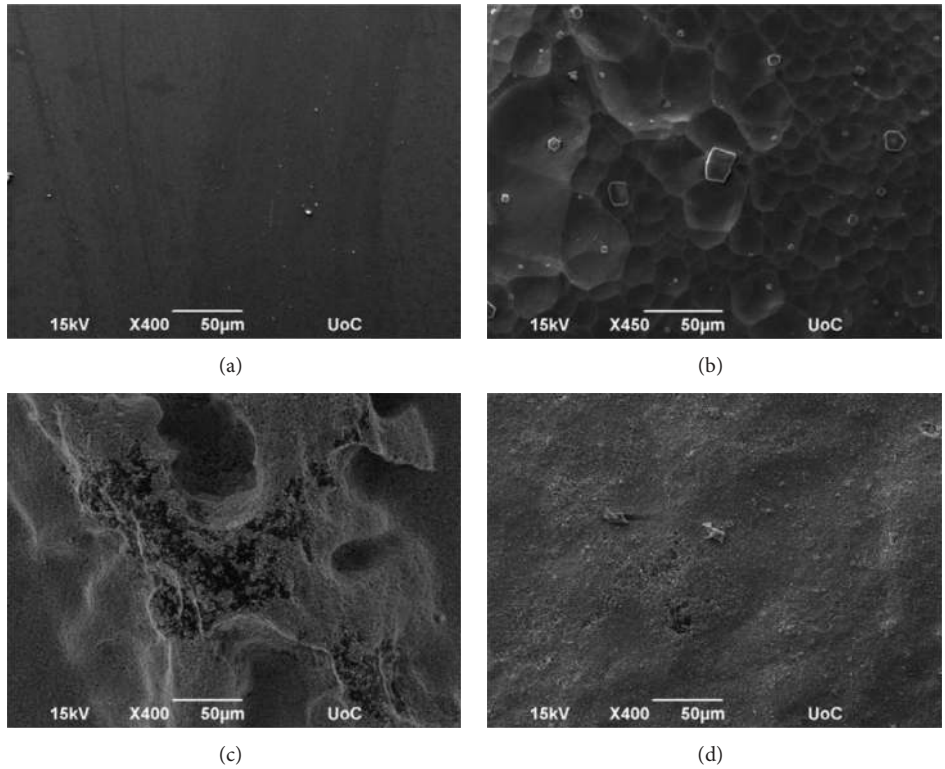

Figure 5: SEM images of (a) glass plates; (b) glass plates treated with HF solution; (c) 3.7 mg fresh ZnO (1.6 mg/cm^2) immobilized onto the plate; and (d) 3.7 mg used ZnO (1.6 mg/cm^2) immobilized onto the plate.

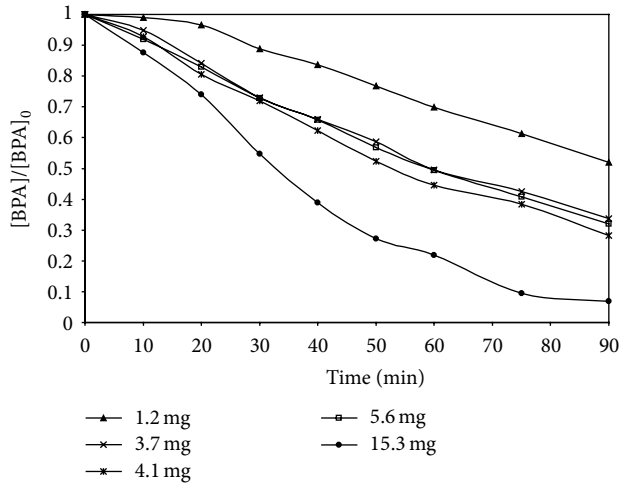

Figure 6: Effect of ZnO loading on the conversion of 100 μg/L BPA in UPW.

powder onto the appropriate substrate. Nevertheless, this does not seem to affect the catalytic activity of ZnO which, on a catalyst-loading basis, is more efficient than TiO_2; for example, a common BPA conversion can be achieved after 90 min at 1.8 mg/cm^2 ZnO or 45.2 mg/cm^2 TiO_2, as can be observed from Figures 3 and 6.

3.3. Effect of Initial BPA Concentration. The effect of initial BPA concentration (50, 100, and 200 μg/L) on its degradation over 150.7 mg/ cm^2 TiO_2 was investigated and concentration-time profiles were followed (data not shown). The 90 min BPA removal was 77 ± 3% irrespective of the initial BPA concentration, thus implying first-order kinetics, that is,

$$-\frac{d\,[\mathrm{BPA}]}{dt} = k_{\mathrm{app}}\,[\mathrm{BPA}] \Longleftrightarrow \ln\frac{[\mathrm{BPA}]_o}{[\mathrm{BPA}]} = k_{\mathrm{app}}t \Longleftrightarrow \ln(1-X) = -k_{\mathrm{app}}t, \tag{3}$$

where k_{app} is an apparent reaction rate constant and X is BPA conversion independent of its initial concentration $[\mathrm{BPA}]_o$.

Figure 7(a) confirms that the reaction approaches, indeed, first-order kinetics. Plotting the logarithm of normalized BPA concentration against time results in straight lines (the coefficient of linear regression of data fitting, r^2, is between 99.3% and 99.6%) with a nearly common slope, which corresponds to the apparent reaction rate constant; this is 15 ± 1 10^{-3} min^{-1}.

The effect of initial BPA concentration was also studied at 1.6 mg/cm^2 ZnO; the 90 min removal was 64±2% irrespective of the initial concentration. Figure 7(b) shows the respective first-order degradation kinetics, from which the apparent rate constant is computed at 11 ± 1 10^{-3} min^{-1} (the coefficient of linear regression of data fitting, r^2, is between 99.4% and 99.6%).

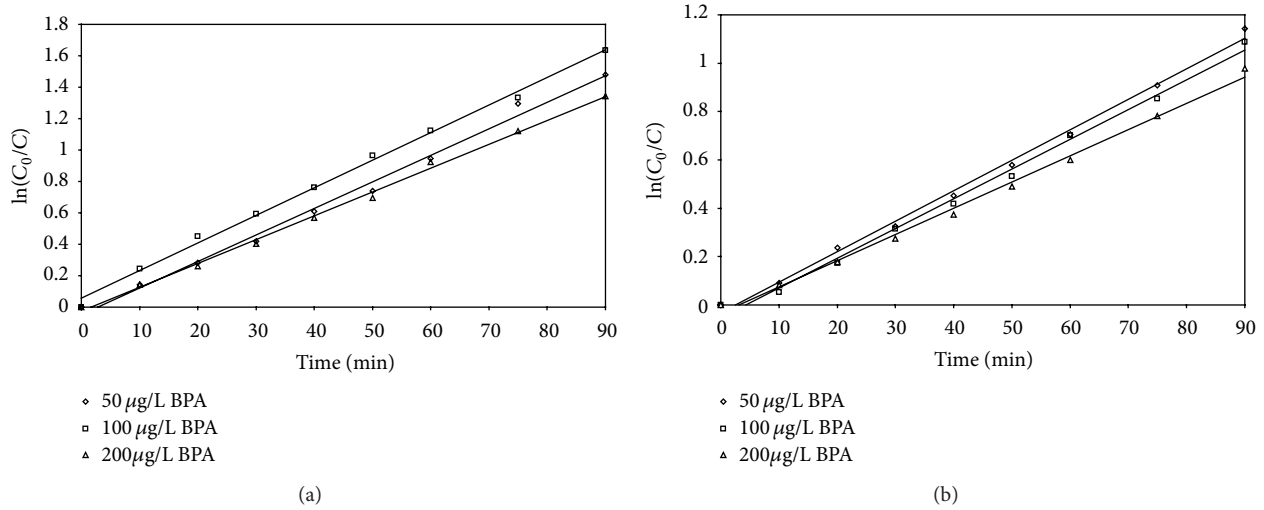

Figure 7: Effect of initial BPA concentration on its degradation in UPW at (a) 150.7 mg/cm^2 TiO_2 and (b) 1.6 mg/cm^2 ZnO. Plot of (3).

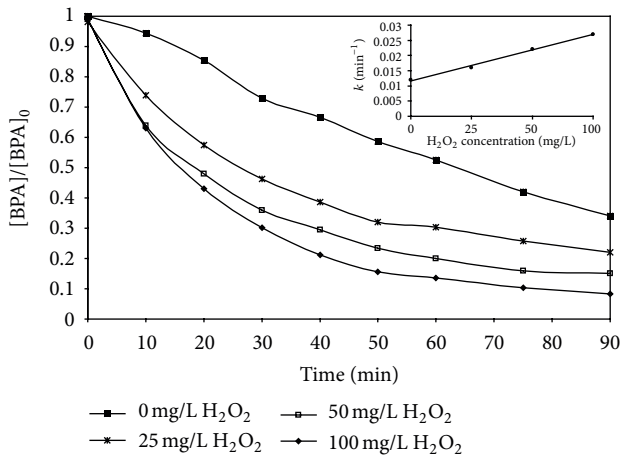

Figure 8: Effect of H_2O_2 on the conversion of 100 μg/L BPA in UPW at 1.6 mg/cm^2 ZnO. Inset graph: change of k_{app} with H_2O_2 concentration.

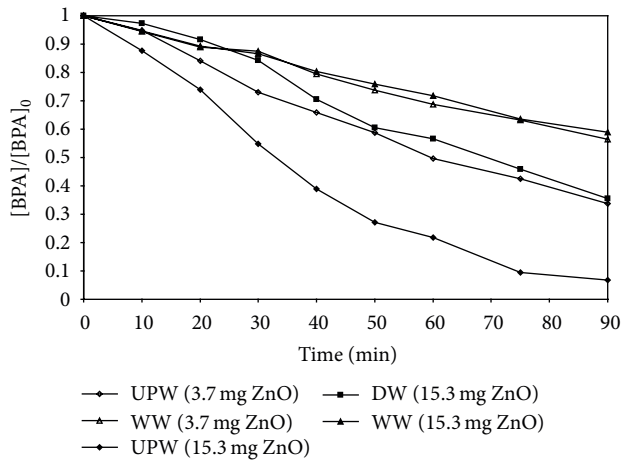

Figure 9: Effect of water matrix on the conversion of 100 μg/L BPA at two ZnO loadings.

From the results presented so far, it is evident that both catalysts exhibit a similar performance for BPA degradation through first-order kinetics. We decided to expand experimentation with ZnO since (a) TiO_2 has extensively been studied in the literature for several environmental applications and (b) ZnO has the potential to achieve improved photocatalytic performance as it absorbs over a wide region of the UV-A spectrum [22]. It should be mentioned here that ZnO is generally more susceptible to photo corrosion and/or chemical corrosion (i.e., leaching) than TiO_2 and this is a point of concern; nonetheless, our previous studies [13] showed that ZnO was remarkably stable during the photocatalytic oxidation of slightly alkaline, wastewater matrices.

3.4. Effect of Hydrogen Peroxide. The addition of oxidizing species increases the efficiency of the photocatalytic process because H_2O_2 is an electron acceptor and reacts with the electrons of the photo-activated surface of the catalyst:

$$H_2O_2 + e^- \longrightarrow {}^{\bullet}OH + OH^- \quad (4)$$

Thus, the addition of peroxide constitutes an extra source of hydroxyl radicals and increases the photoreactivity of ZnO during the photocatalytic degradation [23].

According to our findings (Figure 8), increasing hydrogen peroxide concentration from 0 to 100 mg/L results in increased removal; for example, the 90 min conversion is 66%, 78%, 85%, and 92% at 0, 25, 50, and 100 mg/L H_2O_2, respectively. The inset of Figure 8 shows that the respective apparent rate constants increase almost linearly with the amount of H_2O_2 added up to 100 mg/L.

It should be noted here that H_2O_2 was only partly consumed during the previous photocatalytic runs as confirmed with the peroxide test strips; unfortunately, precise determination of residual peroxide was not possible with this method.

3.5. Effect of Water Matrix. Figure 9 clearly shows that BPA degradation is impeded in complex water matrices

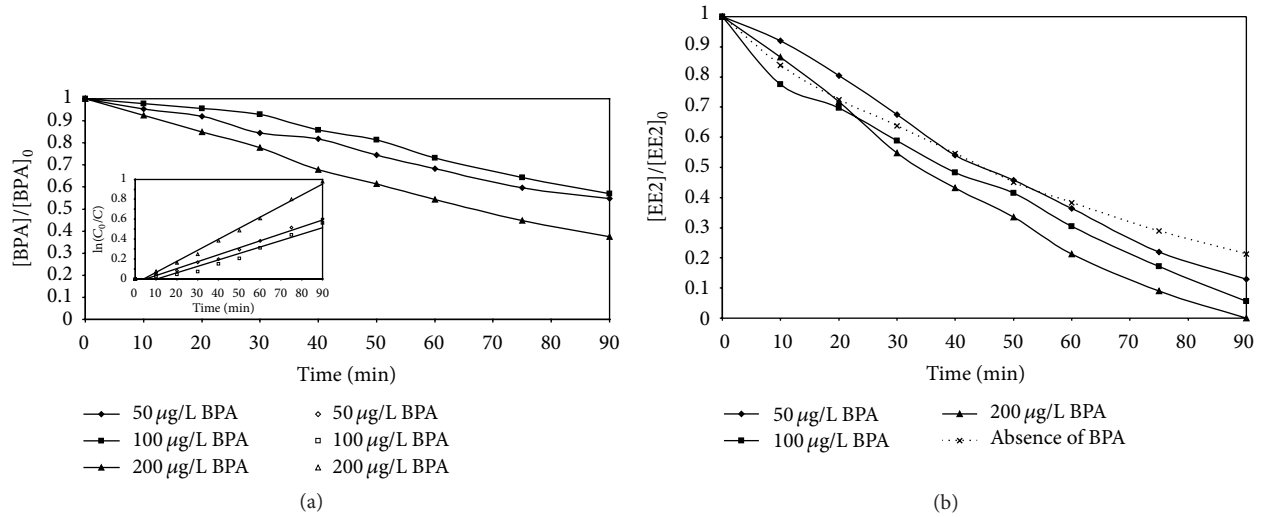

Figure 10: Degradation of a mixture of BPA and EE2 in UPW at 1.6 mg/cm^2 ZnO. Effect of (a) 100 μg/L EE2 on 50, 100 and 200 μg/L BPA; (b) 50, 100 and 200 μg/L BPA on 100 μg/L EE2. Inset graph: plot of (3).

containing organic and inorganic constituents; for instance the 90 min conversion is 93%, 65%, and 41% in UPW, DW, and WW, respectively, at 15.3 mg (6.8 mg/cm^2) ZnO. The respective apparent kinetic constants are computed equal to 0.342 (r^2 = 0.955), 0.128 (r^2 = 0.95), and 0.064 min^{-1} (r^2 = 0.979). The discrepancy by an order of magnitude between kinetics in UPW and WW can be explained taking into account that (a) the oxidizing agents are competitively consumed in reactions involving the residual organic fraction present in treated WW (i.e., COD = 24 mg/L) but not in UPW. Since this is known to be refractory to biological or chemical oxidation [24] and constitutes most of the matrix's total organic content, nonselective oxidizing agents will partly be wasted attacking this fraction; (b) hydroxyl radicals may be scavenged by bicarbonates and chlorides present in WW and/or DW to form the respective radicals, whose oxidation potential is lower than that of hydroxyl radicals [25, 26].

The experiments were repeated at a reduced ZnO loading of 3.7 mg (1.6 mg/cm^2). In this case, the 90 min BPA conversion is 60% in UPW and decreases to 44% in WW with the respective rate constants being 12 10^{-3} min^{-1} (r^2 = 0.994) and 6 10^{-3} min^{-1} (r^2 = 0.992); the ratio k_{UPW}/k_{ww} is 5.3 and 2 at 6.8 and 1.6 mg/cm^2 ZnO, respectively. These results clearly indicate that the degree of deceleration of the photocatalytic process due to the complexity of the water matrix strongly depends on the catalyst-loading.

3.6. Degradation of EDCs Mixture. Experiments were carried out to investigate the possible interactions of BPA with EE2, a synthetic hormone typically found in the contraceptive pill and well-known for its interference with the endocrine system of living beings [27].

Figure 10(a) shows BPA concentration-time profiles (50–200 μg/L initial concentration) in UPW and in the presence of 100 μg/L EE2, while Figure 10(b) shows EE2 concentration-time profiles (100 μg/L initial concentration) in UPW and in the presence of different BPA concentrations in the range 0–200 μg/L. Comparing Figures 7(b) and 10(a) (inset graph), it is deduced that BPA degradation is slightly impeded by the presence of EE2, especially at 50 and 100 μg/L BPA initial concentrations. On the other hand, Figure 10(b) shows an enhancement of EE2 degradation from 79% in the absence of BPA to 87%, 94.5%, and 99% in the presence of 50, 100, and 200 μg/L BPA, respectively. These results are consistent with our previous work [16], where the photocatalytic EE2 degradation was studied in the presence of BPA. Possible explanations of this observation would involve the following (a) differences in BPA and EE2 chemical structures; EE2 has a longer molecular chain with more complicated structure than BPA and this could render it more readily susceptible to oxidative attack; (b) the simultaneous BPA-EE2 degradation may create active radicals that would also attack firstly EE2, facilitating thus its degradation; and (c) EE2, due to its longer and more complex molecule chain, may act as a shield to BPA molecule preventing its diffusion to the catalyst surface, thus decreasing its degradability.

The experiments were then performed in WW and the results are shown in Figure 11. The previous phenomenon is far less pronounced in this case, and this is possibly due to the fact that the WW matrix has already had a strong adverse impact (see Section 3.5), thus masking any interactions between BPA and EE2.

A kinetic simulation of BPA degradation in the presence of EE2 was performed for both UPW and WW matrices. Based on the experimental data shown in Figures 10(a) and 11(a), BPA degradation seems to follow near first-order kinetics as its degradation rate does not depend strongly on its initial concentration. The apparent rate constant for degradation in UPW is 9 ± 2 10^{-3} min^{-1} (computed from the

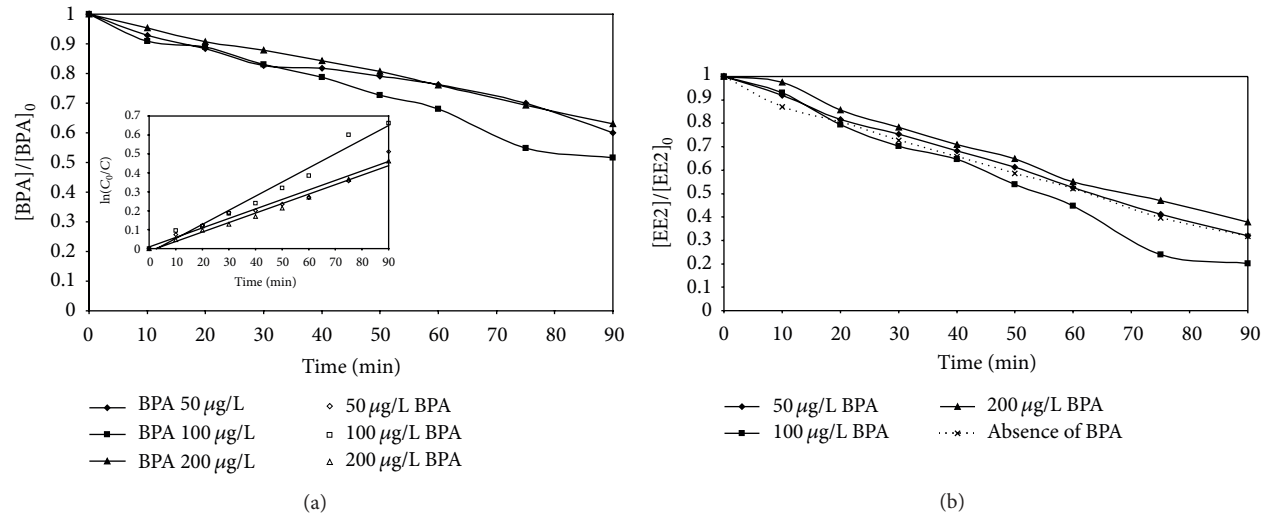

Figure 11: Degradation of a mixture of BPA and EE2 in WW at 1.6 mg/cm^2 ZnO. Effect of (a) 100 μg/L EE2 on 50, 100, and 200 μg/L BPA and (b) 50, 100 and 200 μg/L BPA on 100 μg/L EE2. Inset graph: plot of (3).

slope of the straight lines shown in inset Figure 10(a)) and decreases to $6 \pm 1\ 10^{-3}$ min^{-1} in WW (inset Figure 11(a)).

4. Conclusions

Overall, the removal of BPA under simulated solar irradiation and in the presence of either TiO_2 or ZnO catalysts immobilized onto glass plates was investigated. It was observed that the amount of catalyst attached onto the glass plate can affect process efficiency, which generally increases at increased catalyst loadings under the conditions tested. BPA removal follows a first-order reaction rate indicating that the removal is not practically affected by the initial BPA concentration, in the presence of either TiO_2 or ZnO catalyst. At the conditions employed in this study, apparent reaction rates increase with (a) increasing H_2O_2 concentration in a proportional fashion and (b) decreasing complexity of the water matrix (i.e., from wastewater to drinking water to ultrapure water). The presence of other EDCs, such as EE2, spiked in the reaction mixture does not seem to obstruct BPA degradation.

Hence, solar photocatalytic treatment using immobilized TiO_2 or ZnO photocatalysts can be a promising, with low energy requirements and efficient process to remove endocrine disrupting compounds, found at low concentrations, from aqueous matrices. The key advantage of the proposed setup is that there is no need for catalyst aftertreatment and separation in train with the photocatalytic process, thus decreasing the overall cost of a large-scale treatment plant.

References

[1] P. K. Jjemba, *Pharma-Ecology: The Occurrence and Fate of Pharmaceuticals and Personal Care Products in the Environment*, John Wiley & Sons, Hoboken, NJ, USA, 2008.

[2] V. Belgiorno, L. Rizzo, D. Fatta et al., "Review on endocrine disrupting-emerging compounds in urban wastewater: occurrence and removal by photocatalysis and ultrasonic irradiation for wastewater reuse," *Desalination*, vol. 215, no. 1–3, pp. 166–176, 2007.

[3] C. Lindholst, S. N. Pedersen, and P. Bjerregaard, "Uptake, metabolism and excretion of bisphenol A in the rainbow trout (*Oncorhynchus mykiss*)," *Aquatic Toxicology*, vol. 55, no. 1-2, pp. 75–84, 2001.

[4] H. Barndõk, M. Peláez, C. Han et al., "Photocatalytic degradation of contaminants of concern with composite NF-TiO_2 films under visible and solar light," *Environmental Science and Pollution Research*, vol. 20, no. 6, pp. 3582–3591, 2013.

[5] V. M. Daskalaki, I. Fulgione, Z. Frontistis, L. Rizzo, and D. Mantzavinos, "Solar light-induced photoelectrocatalytic degradation of bisphenol-A on TiO_2/ITO film anode and BDD cathode," *Catalysis Today*, vol. 209, pp. 74–78, 2013.

[6] S. D. Richardson, "Water analysis: emerging contaminants and current issues," *Analytical Chemistry*, vol. 81, no. 12, pp. 4645–4677, 2009.

[7] C. I. Kosma, D. A. Lambropoulou, and T. A. Albanis, "Occurrence and removal of PPCPs in municipal and hospital wastewaters in Greece," *Journal of Hazardous Materials*, vol. 179, no. 1–3, pp. 804–817, 2010.

[8] J. L. Rodríguez-Gil, M. Catalá, S. G. Alonso et al., "Heterogeneous photo-Fenton treatment for the reduction of pharmaceutical contamination in Madrid rivers and ecotoxicological evaluation by a miniaturized fern spores bioassay," *Chemosphere*, vol. 80, no. 4, pp. 381–388, 2010.

[9] G. Gatidou, E. Vassalou, and N. S. Thomaidis, "Bioconcentration of selected endocrine disrupting compounds in the Mediterranean mussel, *Mytilus galloprovincialis*," *Marine Pollution Bulletin*, vol. 60, no. 11, pp. 2111–2116, 2010.

[10] M. Gros, M. Petrović, and D. Barceló, "Tracing pharmaceutical residues of different therapeutic classes in environmental waters by using liquid chromatography/quadrupole-linear ion trap mass spectrometry and automated library searching," *Analytical Chemistry*, vol. 81, no. 3, pp. 898–912, 2009.

[11] A. S. Stasinakis, G. Gatidou, D. Mamais, N. S. Thomaidis, and T. D. Lekkas, "Occurrence and fate of endocrine disrupters in Greek sewage treatment plants," *Water Research*, vol. 42, no. 6-7, pp. 1796–1804, 2008.

[12] M. Auriol, Y. Filali-Meknassi, R. D. Tyagi, C. D. Adams, and R. Y. Surampalli, "Endocrine disrupting compounds removal from wastewater, a new challenge," *Process Biochemistry*, vol. 41, no. 3, pp. 525–539, 2006.

[13] Z. Frontistis, D. Fatta-Kassinos, D. Mantzavinos, and N. P. Xekoukoulotakis, "Photocatalytic degradation of 17α-ethynylestradiol in environmental samples by ZnO under simulated solar radiation," *Journal of Chemical Technology and Biotechnology*, vol. 87, no. 8, pp. 1051–1058, 2012.

[14] M. A. Behnajady, N. Modirshahla, N. Daneshvar, and M. Rabbani, "Photocatalytic degradation of C.I. Acid Red 27 by immobilized ZnO on glass plates in continuous-mode," *Journal of Hazardous Materials*, vol. 140, no. 1-2, pp. 257–263, 2007.

[15] A. R. Khataee, "Photocatalytic removal of C.I. Basic Red 46 on immobilized TiO_2 nanoparticles: artificial neural network modelling," *Environmental Technology*, vol. 30, no. 11, pp. 1155–1168, 2009.

[16] V. Koutantou, M. Kostadima, E. Chatzisymeon et al., "Solar photocatalytic decomposition of estrogens over immobilized zinc oxide," *Catalysis Today*, vol. 209, pp. 66–73, 2013.

[17] T. Nakashima, Y. Ohko, D. A. Tryk, and A. Fujishima, "Decomposition of endocrine-disrupting chemicals in water by use of TiO_2 photocatalysts immobilized on polytetrafluoroethylene mesh sheets," *Journal of Photochemistry and Photobiology A*, vol. 151, no. 1–3, pp. 207–212, 2002.

[18] V. M. Daskalaki, Z. Frontistis, D. Mantzavinos, and A. Katsaounis, "Solar light-induced degradation of bisphenol-A with TiO_2 immobilized on Ti," *Catalysis Today*, vol. 161, no. 1, pp. 110–114, 2011.

[19] J. Gunlazuardi and W. A. Lindu, "Photocatalytic degradation of pentachlorophenol in aqueous solution employing immobilized TiO_2 supported on titanium metal," *Journal of Photochemistry and Photobiology A*, vol. 173, no. 1, pp. 51–55, 2005.

[20] R. Wang, D. Ren, S. Xia, Y. Zhang, and J. Zhao, "Photocatalytic degradation of Bisphenol A (BPA) using immobilized TiO_2 and UV illumination in a horizontal circulating bed photocatalytic reactor (HCBPR)," *Journal of Hazardous Materials*, vol. 169, no. 1–3, pp. 926–932, 2009.

[21] E. S. Galbavy, K. Ram, and C. Anastasio, "2-Nitrobenzaldehyde as a chemical actinometer for solution and ice photochemistry," *Journal of Photochemistry and Photobiology A*, vol. 209, no. 2-3, pp. 186–192, 2010.

[22] M. A. Behnajady, N. Modirshahla, and R. Hamzavi, "Kinetic study on photocatalytic degradation of C.I. Acid Yellow 23 by ZnO photocatalyst," *Journal of Hazardous Materials*, vol. 133, no. 1–3, pp. 226–232, 2006.

[23] F. Méndez-Arriaga, M. I. Maldonado, J. Gimenez, S. Esplugas, and S. Malato, "Abatement of ibuprofen by solar photocatalysis process: enhancement and scale up," *Catalysis Today*, vol. 144, no. 1-2, pp. 112–116, 2009.

[24] Z. Frontistis and D. Mantzavinos, "Sonodegradation of 17α-ethynylestradiol in environmentally relevant matrices: laboratory-scale kinetic studies," *Ultrasonics Sonochemistry*, vol. 19, no. 1, pp. 77–84, 2012.

[25] L. A. T. Espinoza, M. Neamţu, and F. H. Frimmel, "The effect of nitrate, Fe(III) and bicarbonate on the degradation of bisphenol A by simulated solar UV-irradiation," *Water Research*, vol. 41, no. 19, pp. 4479–4487, 2007.

[26] C. Sirtori, A. Agüera, W. Gernjak, and S. Malato, "Effect of water-matrix composition on trimethoprim solar photodegradation kinetics and pathways," *Water Research*, vol. 44, no. 9, pp. 2735–2744, 2010.

[27] Z. Frontistis, C. Drosou, K. Tyrovola et al., "Experimental and modeling studies of the degradation of estrogen hormones in aqueous TiO_2 suspensions under simulated solar radiation," *Industrial and Engineering Chemistry Research*, vol. 51, no. 51, pp. 16552–16563, 2012.